CELLULOSE HYDROGEL FIBRE FROM NIPA PALM (*NYPA FRUTICANS*) SHELL USED FOR ADSORPTION OF METHYLENE BLUE FROM WASTEWATER

KHOA DANG NGUYEN

Faculty of Environment, School of Engineering and Technology,
Van Lang University, 69/68 Dang Thuy Tram Str., Ward 13, Binh Thanh District,
Ho Chi Minh City, Vietnam
✉ *Corresponding author: khoa.nd@vlu.edu.vn*

Received March 21, 2022

Cellulose was chemically extracted from nipa palm (*Nypa fruticans*) shell, which was used to prepare hydrogel fibre and applied as an environment-friendly adsorbent for methylene blue. The purified cellulose was dissolved in *N,N*-dimethylacetamide (DMAc), with the addition of 6% lithium chloride (LiCl), at room temperature for 5 days. Then, the cellulose solution was coagulated by the phase inversion process under ethanol vapor to obtain cellulose hydrogel fibre. The adsorption results showed that when the initial concentration of the methylene blue solution was increased from 20 to 100 mg/L at pH 10, the adsorption capacity also rose from 3 to 11.53 mg/g after 15-minute immersion. In addition, the equilibrium adsorption isotherm was well-fitted to the Langmuir isotherm model and the maximum adsorbed amount was 13.23 mg/g. Furthermore, the cellulose hydrogel fibre showed high reusability, as the removal efficiency of methylene blue remained at a level of approximately 80% after five recycles.

Keywords: adsorption, cellulose, hydrogel, methylene blue, nipa palm

INTRODUCTION

In recent years, the intense development of the textile dyeing industry in Vietnam has contributed greatly to the country's overall economic development. The textile dyeing industry does not only meet the needs of domestic consumption, but also brings great economic value from exports. Besides, the textile dyeing industry also creates jobs for a large labour force. However, most textile processing wastewater has high alkalinity and colorants, thus large amounts of chemicals are discharged directly into rivers, streams, ponds, lakes *etc*. Such wastewater is toxic to aquatic species. Therefore, it is necessary to treat dye-contaminated wastewater prior to discharging it into the environment by conventional processes, such as chemical precipitation,[1] ion exchange,[2] advanced oxidation,[3] and electrochemical processes.[4] However, these processes have significant disadvantages, for instance, incomplete removal, high energy requirements, chemical agents and massive production of toxic sludge.[5]

Dye adsorption has been in the research focus in recent years due to its significant advantages in wastewater treatment. Various agricultural by-products have been investigated as adsorbents for the removal of dyes from wastewater.[6] Using low-cost alternative adsorbents to the expensive carbon materials is important due to its double benefits, in water treatment and in waste management.[7] Among the adsorption techniques, biosorption uses an inactive (non-living) sorbent of biological origin to bind different organic substances, including dye ions. Several functional groups, such as hydroxyls and amines in biopolymer-based adsorbents are able to increase the removal of the dye.

As a biopolymer, cellulose is the most abundant polysaccharide in nature, the major source of cellulose being plant fibre (Fig. 1a). Approximately 40% of the plant composition represents cellulose, which serves as a solid structural fraction within the complex architecture of cell walls. Independently of its source, cellulose consists of D-glucopyranose ring units.

It possesses various systems of hydrogen bonds, which have a significant influence on its properties. For instance, the limited solubility of cellulose in most solvents, the reactivity of the hydroxyl groups, and the crystallinity of cellulose samples originate from robust hydrogen bonding systems. Cellulose also contains hydrophobic areas (around the C atoms) that influence the overall properties, including solubility.[8] It is known that the lithium chloride (LiCl)/*N,N*-dimethylacetamide (DMAc) solvent system can increase the solubility of polysaccharide segments.[9] Then, a phase inversion process can be used to prepare a cellulose hydrogel at room temperature under ethanol vapour, without using cross-linker chemicals[10-12] In terms of potential adsorbents for water treatment, biopolymer-based hydrogels are hydrophilic, which means they can store a vast amount of water inside their polymeric network.[13] Therefore, biopolymer-based hydrogels have been demonstrated as potential materials with high dye removal ability.[14,15]

Also, in applying adsorbents to remove contaminants from water, the shape of the materials plays an important role, as the adsorption capacity of the material depends on its surface area. Hydrogel fibre is a hydrogel having a fibrous shape, where the width or diameter is significantly smaller than the length. Therefore, the specific surface area for the fibrous state of the mentioned hydrogel is more significant than that of the bulk hydrogel. As a result, it is expected that hydrogel fibre will exhibit favourable mass transfer at a faster exchange rate. Hence, fibre-based hydrogels can be attractive adsorbents, owing to their high surface-to-volume ratio and adsorption rate.[16]

Nipa palm (*Nypa fruticans*) is a useful, versatile and common component of mangrove forests in Asia and Oceania. In addition to a host of local subsistence uses, ranging from medicines to hats and raincoats, some important commercial uses have led to management efforts and have triggered renewed interest in its potential.[17] The flesh of nipa palm (*Nypa fruticans*) is white, soft, sweet, aromatic, cool, and it is edible, helping to cool and quench thirst. After extracting the nipa palm flesh, the huge amounts shells remaining as a by-product could be used as a biopolymer source. As reported, the chemical composition of nipa palm shells is the following: cellulose (45.6%), hemicelluloses (23.5%), lignin (19.4%), protein (0.8%), ash (8.2%) and others (1.3%).[18] Therefore, in the present work, nipa palm shells were considered for cellulose extraction for the preparation of hydrogel fibres by the phase inversion method. Then, the obtained cellulose fibre was applied as an adsorbent for methylene blue from wastewater and the reusability of this material was evaluated.

EXPERIMENTAL

Materials

Nipa palm (Nypa fruticans) fibres were collected from Can Gio District, Ho Chi Minh City. All chemicals used were of analytical grade. Methylene blue was purchased from Merck, Germany. Hydrochloric acid (HCl), nitric acid (HNO_3), sodium hydroxide (NaOH), potassium hydroxide (KOH), *N,N*-dimethylacetamide (DMAc), lithium chloride (LiCl) and ethanol were obtained from Nacalai Tesque, Inc. (Tokyo, Japan). Prior to using DMAc, KOH was placed in the solvent and stored over five days and LiCl was dried at 80 °C overnight to remove traces of moisture. Other chemicals were used without any further purification.

Pretreatment of nipa palm (Nypa fruticans) fibres and extraction of cellulose

The collected nipa palm (*Nypa fruticans*) fibres (NPF) were washed with an excess amount of water to remove all traces of dirt, followed by drying under sunshine for 24 h, and then were cut to the size of 1-2 cm.

For cellulose extraction from NPF, about 10 g of the size-reduced fibres were suspended in 300 mL of 0.5 M NaOH aqueous solution for 24 h at room temperature for the alkali treatment. The obtained black slurry was filtered and washed with excess distilled water until neutral pH, to eliminate traces of NaOH. Then, the alkaline-treated NPF were refluxed by adding them to 300 mL of a mixture of ethanol and HNO_3 (4:1 in vol%) at 60 °C for 3 h, while the chemical mixture was replaced once each hour. Finally, the pretreated NPF were washed with excess distilled water to eliminate traces of ethanol and HNO_3, and then oven-dried for 3 h at 90 °C. The extraction percentage of cellulose (NPC) from NPF was calculated by the following equation:

$$\text{Yield (\%)} = m \times 100 / m_0 \quad (1)$$

where m_0 (g) is the initial amount of NPF and m (g) is the dry weight of the fibres after the chemical treatment (NPC).

The dried NPC was further used for characterizations and preparation of the cellulose solution.

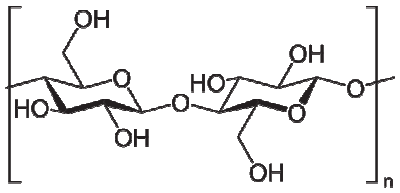

(a)

(b)

Figure 1: Chemical structure of cellulose (a) and nipa palm *(Nypa fruticans)* shell (b)

Methods

Preparation of cellulose solution and cellulose hydrogel fibres

Before dissolving, NPC was prepared in three steps of solvent exchange. First, the NPC was suspended in 300 mL of distilled water under stirring for 24 h at 180 rpm, to allow the pretreated NPF to swell and lose its cellulose structure. Afterward, the water swollen NPC was filtrated by a filter. Then, the swollen NPC was stirred in 300 mL of ethanol at room temperature for 24 h at 180 rpm and filtrated. Finally, the NPC was stirred in 300 mL of DMAc at room temperature for 24 h at 180 rpm and filtrated. About 1 g of the obtained swollen NPC was placed in 6% DMAc/LiCl solution and stirred at room temperature for about five days to obtain a homogeneous viscous solution. Following that, the cellulose solution was centrifuged at 6000 rpm for 20 minutes to remove the undissolved parts. After that, the cellulose solution was obtained in about 1% concentration.

For the preparation of the cellulose hydrogel fibres (CHF), about 10 g of the viscous cellulose solution was poured into the mould having the cylindrical shape with 0.5 cm in diameter and 25 cm in length. The mould containing the cellulose solution was placed in a plastic container filled with 40 mL of ethanol for the phase inversion process for 24 h at room temperature. After that, the cellulose hydrogel fibre was washed in an excess amount of distilled water to remove traces of solvent before further measurements.

Evaluation of extracted cellulose and cellulose hydrogel fibre

Fourier-transform infrared (FT-IR) spectra were recorded with a Jasco FT-IR/4100 spectrometer, in the absorbance mode, from 4000 to 500 cm^{-1} wavelengths, with the resolution of 2 cm^{-1}. The samples were prepared by grinding dried NPF, pretreated NPF and CHF, and mixing each with potassium bromide (KBr).

Scanning electron microscopy (SEM) was used to examine the cross-section morphology of the CHF. For the measurement, the CHF samples were fractured in liquid nitrogen and freeze-dried for 24 h. Then, the samples were gold sputtered for the formation of a conductive layer (JSM-5300LV JEOL, Japan).

Adsorption of methylene blue onto CHF

Effect of pH

Batch adsorption experiments using the CHF were conducted under various pH conditions. About 0.1 g of CHF was placed in 20 mL of MB with the initial concentration of 50 mg/L, and shaken at room temperature, with constant speed at 180 rpm. The pH was adjusted from 2 to 12 by NaOH 1N and HCl 1N aqueous solution. After two hours, the CHF was removed, and the remaining concentration of the MB solution was determined by a UV-Vis spectrophotometer at 664 nm.

Effect of contact time

Besides the pH, contact time is another factor that greatly affects the adsorption capacity of a material. Herein, contact time experiments were carried out from 15 to 240 minutes. The dosage of CHF was 0.1 g with the initial concentration of MB was 50 mg/L at pH of 10.

The kinetic adsorption of MB by CHF was investigated by the pseudo-first-order (PFO) and pseudo-second-order (PSO) models, according to the following equations:[19]

$$Ln(q_e - q_t) = Lnq_e - k_1 t \quad (2)$$

$$\frac{1}{q_t} = \frac{1}{k_2 q_e^2} + \frac{t}{q_e} \quad (3)$$

where q_e is the mass of adsorbate per unit mass of adsorbent at equilibrium; q_t is the mass of adsorbate per unit mass of adsorbent at time t; k_1 is the PFO rate constant (1/h) and k_2 is the PSO rate constant (g/(mg.h)).

Effect of initial concentration

The initial concentration of the contaminant solution greatly influenced the maximum adsorption capacity of the material. Initial concentrations of MB of 20, 40, 50, 60, 80 and 100 mg/L were used for a contact time of 15 minutes, at pH 10 and the amount of the CHF was 0.1 g.

The dried CHF was immersed into 20 mL of MB at room temperature to study the adsorption equilibrium. Upon the completion of the pre-set time intervals, the concentration of MB in the aqueous solution was measured. The adsorption amount at the current time (qt, mg/g) and equilibrium adsorption capacity (q_e, mg/g) were calculated according to the following equation:

$$q_{t,e} = \frac{(C_0 - C_{t,e}) \times V}{M} \quad (4)$$

where C_o and C_t (mg/L) are the concentrations of the solution at the initial time and time t (h), respectively; C_e (mg/L) is the equilibrium concentration of MB solution; V (L) is the volume of the contaminated solution and m (g) is the weight of the dried CHF.

The Langmuir and Freundlich models were selected to illustrate the relationship between the residual concentration of MB dye in solution and the adsorption capacity of CHF at constant temperature.

The linear equation of the Langmuir isotherm model was used as in the equation below:

$$\frac{C_e}{q_e} = \frac{1}{K_L q_m} + \frac{C_e}{q_m} \quad (5)$$

where q_m (mg/g) is the maximum adsorption capacity, and K_L (L/mg) is the Langmuir constant.

The linear equation of the Freundlich isotherm model is presented as follows:

$$\ln q_e = \ln K_F + \frac{1}{n} \ln C_e \quad (6)$$

where K_F (mg/g) and n are the Freundlich isotherm constants related to the adsorption capacity and to the adsorption strength, respectively.

Desorption and reusability of CHF

After the adsorption at 50 mg/L of initial concentration, pH 10, for 15 minutes at room temperature, the CHFs were collected and dried at 90 °C for 24 h. After that, about 0.1 g of MB-loaded CHFs was immersed in 300 mL of 0.1 N HCl aqueous solution and stirred at 180 rpm. The released amounts of MB were measured at different times of 15, 30, 45, 60, 90, 120 minutes to determine the optimum desorption time of the MB-loaded CHFs. For the reusability experiment, about 0.1 g of the desorbed CHFs was placed in 20 mL of 50 mg/L MB solution, adjusted to pH 10, under stirring at 180 rpm at room temperature. After 15 minutes, the CHFs were removed and the remaining concentration of MB was measured by a UV-Vis spectrometer at the wavelength of 664 nm.

RESULTS AND DISCUSSION

Appearance of the extracted cellulose (NPC) from NPF

The purification of NPC could be carried out through alkaline immersion in a NaOH aqueous solution and reflux treatment in HNO_3/ethanol mixtures, which eliminated the traces of sugars, ash, pigment and lignin, as well as hemicelluloses. According to R.G. Candido *et al.*, the refluxing treatment with acid could remove the hemicellulose and lignin content in amounts of 70.78% and 52.22%, respectively.[20] As seen in Figure 2, the colour of the NPF was brown (a), while the appearance of NPC was white (b). The obtained cellulose extracted from NPF was softer than the raw material due to the removal of lignin and hemicelluloses from the material's composition. However, parts of cellulose may have been removed as well. In this study, the yield of NPC was about 25.6%. In addition, the CHF was yellow, with a diameter of 1 cm, as can be noted in Figure 2 (c).

(a) (b) (c)

Figure 2: NPF (a), NPC (b) and CHF (c)

FT-IR and SEM analyses

Figure 3 shows the FT-IR spectra of NPF and NPC. As seen in both samples, similar peaks were observed at 3380 cm^{-1} assigned to –OH, at 2911 cm^{-1} representing C–H stretching, and at 900-1200 cm^{-1} standing for C–O–C and C–O in the biomass structure. The vibration at 1645 cm^{-1} represented the –OH in the free water, indicating the hydrophilicity of the cellulose. In the case of the raw NPF, the presence of hemicelluloses and

lignin was suggested by the presence of C=O and C–H groups at the wavelengths of 1540 cm^{-1} and 1725 cm^{-1}, respectively.[21] However, after chemical processing, the NPF shows a reduction in the intensity of these vibrations, indicating a loss of these components in the raw materials. Therefore, the purification of cellulose from NPF was well-conducted. Figure 3 also presents the FT-IR spectrum of CHF. The vibrations of the functional groups in CHF and NPC were noted, which means the chemical structure remained unchanged after the preparation of CHF from the NPC solution by phase inversion under ethanol vapor.

The microstructure of CHF was observed by SEM, and the micrographs are shown in Figure 4. The results indicate that the cross-sectional structure of the CHF was stratified and tightly packed. As seen in Figure 4 (a), the image at 200× magnification suggests the size of the CHF was about 937.5 µm in diameter.

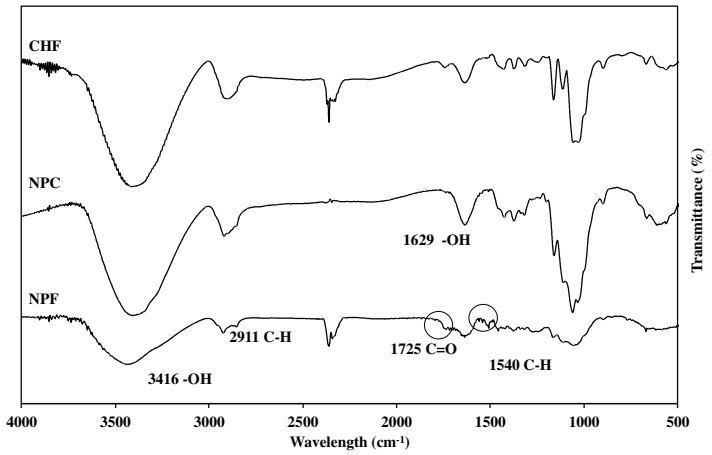

Figure 3: FT-IR spectra of NPF, NPC and CHF

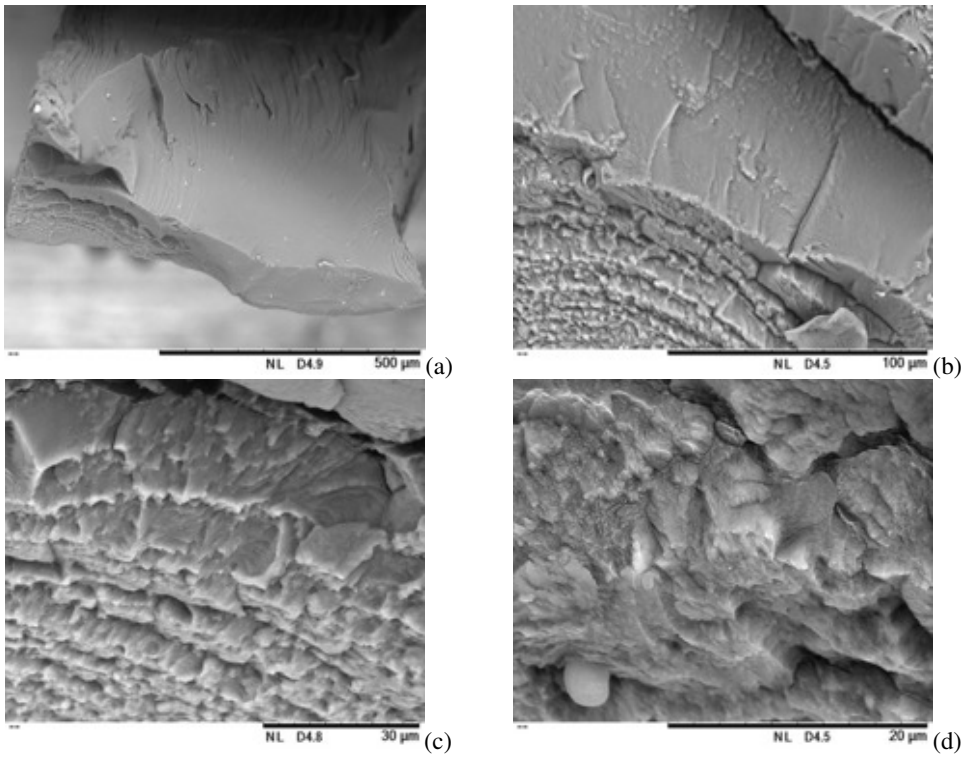

Figure 4: SEM micrographs of the crossectional area of CHF at 200× (a), 1000× (b), 2000× (c) and 5000× (d)

In addition, at 1000× and 2000×, there were several cracks stretching within the stratified structure. The roughness of the cross-section of the CHF was also visible at 5000× magnification. This evidenced that the solvent exchange between DMAc and ethanol was conducted during the phase inversion process, indicating the cellulose solution transformed into a fibre shape in the solid state, in the mould forming CHF. Therefore, this structure of CHF makes it potentially useful as an adsorbent in solutions.

Adsorption experiment with CHF in MB aqueous solution

Effect of pH

The pH is considered one of the most critical factors of the surrounding environment that influence the adsorption capacity of the material. At low pH, due to high concentration of H+ ions, the surface of the adsorbent is positively charged, thus these H^+ ions formed in the aqueous solution are able to compete with other MB cation ions. As a consequence, the interaction that takes place is electrostatic repulsion, reducing the adsorption of MB to the surface of the material. On the contrary, in a high pH environment, a negatively charged surface of the adsorbent is formed due to the OH– available, increasing the adsorption capacity of CHF for MB. It may indicate that the removal of MB by CHF was caused by the electrostatic interaction between the hydroxyl groups of CHF and MB cations. As seen in Figure 5, the adsorbed amount of MB onto CHF increased from 6.88 mg/g to 7.88 mg/g, when the pH rose from 2 to 10. However, the binding capacity of MB to CHF decreased at pH 12 with 7.14 mg/g. Therefore, the most suitable pH in this study was found to be 10.

Effect of contact time

Contact time is another factor affecting the adsorption process. It is necessary to determine the saturation capacity of the material after a certain period of time. The adsorption capacity was noticed to increase slightly from 7.85 mg/g to 8.0 mg/g when contact time rose from 15 min to 120 min. After that, the CHF reached an equilibrium state, leading to a gradual decrease in the adsorption capacity from 120 minutes to 240 minutes, specifically from 8.00 mg/g to 7.61 mg/g. Therefore, it was considered that the optimum time contact was 15 minutes, as seen in Figure 6.

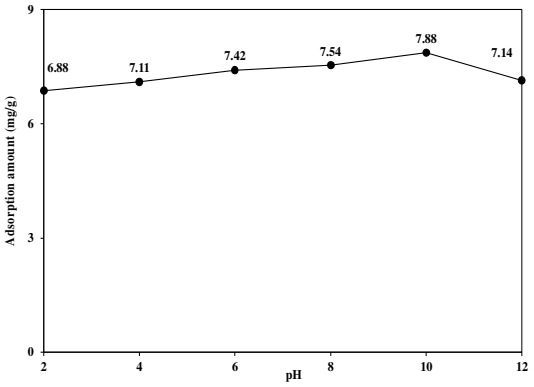

Figure 5: Adsorbed amount (mg/g) of MB onto CHF as a function of pH

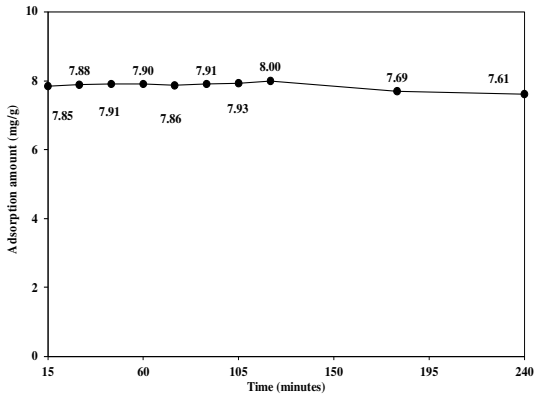

Figure 6: Adsorbed amount (mg/g) of MB onto CHF as a function of contact time

The kinetic models were evaluated to clarify the adsorption behaviour of MB ions onto CHF. When the contact time increased, the remaining vacant sites were difficult to occupy by the dye ions, and the adsorption process reached equilibrium. Kinetic parameters were shown in Table 1, and the linear fitting was shown in Figure 7 (b). The correlation coefficient (R^2) for the pseudo-first-order (PFO) model was 0.4713, which was lower than that for the pseudo-second-order one (PSO). On the other hand, the q_e of 7.92 mg/g calculated from the PSO model was close to the experimental value of 7.93 mg/g. This evidenced that the adsorption of MB onto CHF in the present study was described better by PSO and it occurred mostly by the surface complexation reaction between the cationic dye and the negatively charged sites on the CHF.[19]

Effect of initial concentration

The initial concentration is an essential factor in investigating the adsorption process of MB. Based on the pH and contact time results, the influence of the initial concentration was investigated.

The Langmuir and Freundlich isotherm models were applied to determine the way the adsorption onto CHF takes place, based on the linear coefficients of these equations. As seen in Figure 8, the initial concentration of MB had a strong effect on the bound amount of MB onto CHF. When the concentration was changed from 20 to 100 mg/L, the adsorption capacity increased from 3 to 11.53 mg/g, respectively. It indicated that higher concentration of MB in the initial solutions may not be refused by the adsorption sties in the CHF structure.

Based on the results for the effect of initial MB concentration on the adsorption onto CHF, the adsorption isotherm was obtained to determine the parameters of the two models. As seen from the linearity of the plots in Figure 9, the correlation coefficient (R^2) was 0.994 for the Langmuir model, almost close to one, meaning that this model provided a good fit to the MB adsorption data. On the other hand, the value of R^2 obtained for the Freundlich model was lower – 0.8405 (Fig. 10). Therefore, the Langmuir isotherm model fitted the experimental results better, which meant that the adsorption of MB onto the CHF was a monolayer process, taking place at specific homogeneous sites within the adsorbent and all the adsorption sites were energetically identical.[22] The values of the parameters for the adsorption isotherm are listed in Table 2. As seen in Figure 11, the adsorption isotherm fitted well the experimental results and the maximum adsorbed amount q_m was 13.22 mg/g.

Table 1
Kinetic parameters of PFO and PSO for MB adsorption to CHF

Pseudo-first-order (PFO)			Pseudo-second-order (PSO)		
q_e (mg/g)	k_1 (1/h)	R^2	q_e (mg/g)	k_2 (g/mg.h)	R^2
0.15	0.3457	0.4731	7.92	0.025	0.9999

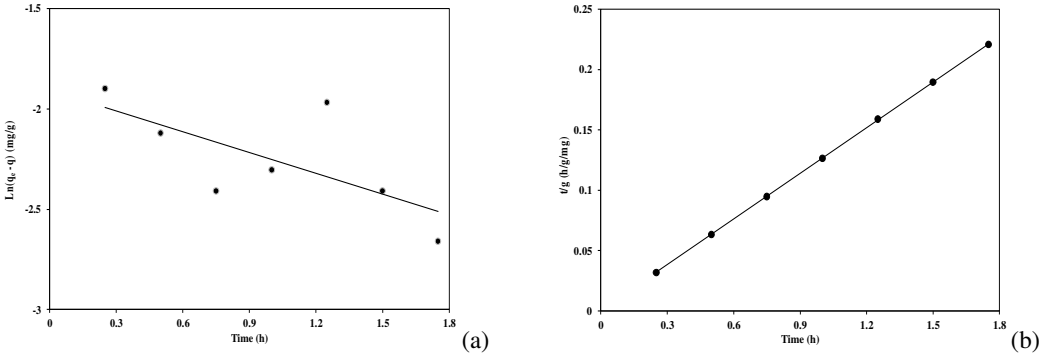

(a) (b)

Figure 7: Pseudo-first-order (a) and pseudo-second-order (b) kinetic linear models

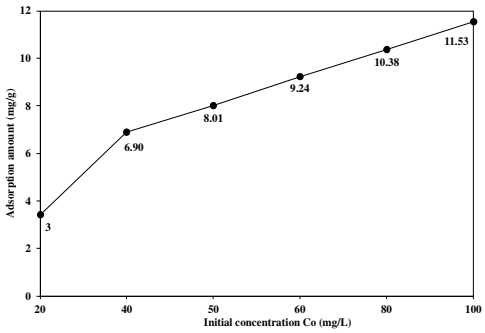

Figure 8: Adsorbed amount (mg/g) of MB onto CHF as a function of initial MB concentration

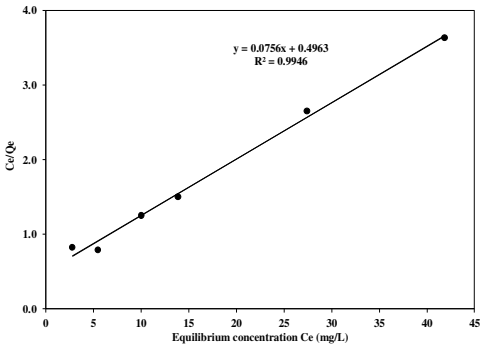

Figure 9: Langmuir linear isotherm for adsorption of MB onto CHF

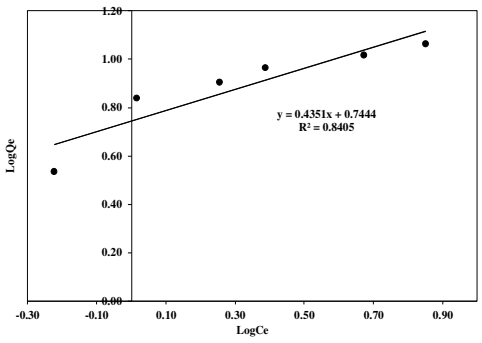

Figure 10: Freundlich linear isotherm for adsorption of MB onto CHF

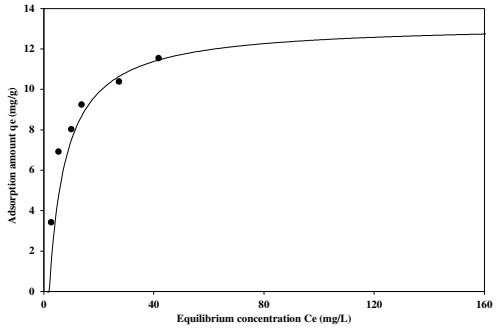

Figure 11: Adsorption isotherm of MB to CHF

Table 2
Adsorption isotherm parameters for MB adsorption to CHF

Model	Parameters				
	q_m (mg/g)	k_L (L/mg)	K_F (L/g)	1/n	R^2
Langmuir	13.22	0.1611	-	-	0.9946
Freundlich	-	-	5.55	0.7444	0.8405

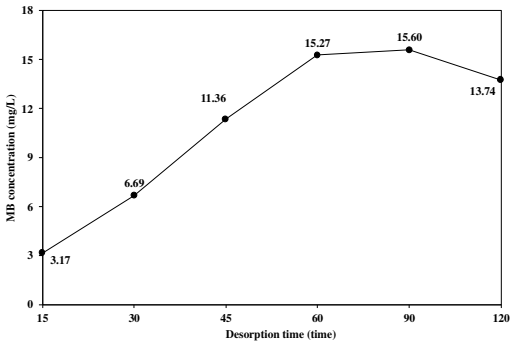

Figure 12: Effect of desorption time on the released concentration of MB

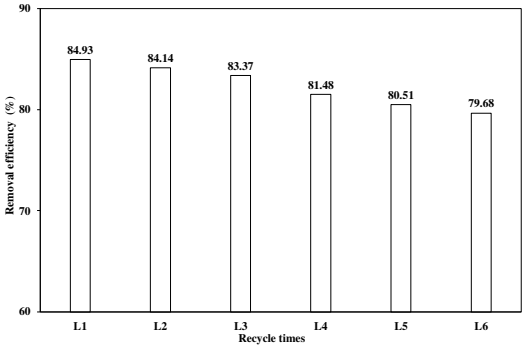

Figure 13: Effect of recycling times on removal efficiency (%) of MB

Desorption and regeneration of CHF

As seen in Figure 12, the releasing concentration of MB was dependent on desorption time, while using acid as an elute. During the elution process, the H^+ cations in the HCl aqueous solution replaced the MB cations adsorbed by CHF. When increasing the desorption time from 15 to 60 minutes, the MB concentration released from the CHF adsorbent rose from 3.17 to 15.27 mg/g. After that, the MB concentration decreased from 15.6 mg/g for 90 minutes desorption time to 13.74 mg/g for 120 minutes desorption time. It may be explained by the lack of sufficient acid concentration after the

desorption time exceeded 90 minutes. According to these results, the desorption time was fixed at 60 minutes in this study.

The reusability of an adsorbent is one of the crucial criteria determining its value. In this study, a number of desorption cycles were performed to examine the regeneration characteristics of the CHF adsorbent.[22] The results shown in Figure 13 suggest that the adsorption capacity remained around 80% after six adsorption/desorption cycles. These results revealed that the prepared CHF could be repeatedly used for MB removal, due to its excellent reusability, recommending the CHF as a promising absorbent.

Comparison with other adsorbents

The adsorption of methylene blue has been extensively studied using the most diverse materials, including a variety of low-cost adsorbents developed from agricultural residues. Table 3 allows a comparison of the adsorption parameters, *i.e.* initial concentration of MB, contact time and uptake of MB, obtained in the present study with those found for other adsorbents reported in the literature.

It should be remarked that, even though there have been many studies on biomass-based adsorbent materials, a notable advantage of CHF is related to its fibre shape, which has been found to be attractive due to its high surface-to-volume ratio. Due to this property, hydrogel fibres exhibit favourable mass transfer, offering distinct benefits for different applications.[23] As can be seen from our findings, the CHF prepared in this study showed more rapid saturation time in the adsorption of MB. Coupled with its high reusability, these properties recommend the CHF as a promising material for MB removal from polluted wastewater. Moreover, CHF was developed from *Nypa fruticans* shells – an abundant resource, which is not valorised properly at present. This makes CHF a low-cost and environmentally friendly adsorbent.

Table 3
Comparison of initial concentration of MB, contact time and maximum adsorption uptake of MB onto CHF and other reported adsorbents

Adsorbent	Initial concentration of MB (mg/L)	Contact time (min)	Adsorption uptake of MB (mg/g)	Reference
Pure cellulose	19.19	80	0.11	[24]
Moroccan Thuya lignin	19.19	140	3.55	[25]
Algerian date stones	100	60	4.9	[26]
Cellulose acetate	50	1440	4.9	[27]
Cellulose hydrogel fiber	50	15	7.85	This study
Crosslinked cellulose hydrogel	50	300	19.03	[28]
Populus tremula cellulose	50	20	35	[29]

CONCLUSION

A cellulose hydrogel fiber was successfully developed from cellulose extracted from nipa palm shells by phase inversion, and then used for the adsorption of MB from aqueous solution. The fiber preparation, involving a mixing process with ethanol vapor and 6% LiCl/DMAc solvent system, provided a stratified and tightly packed crossectional area of the CHF. In the MB adsorption study, the experimental results suggested that the adsorption behaviour was best described by the Langmuir model, the maximum MB uptake being of 13.22 mg/g at pH 10, with saturation time established at 15 minutes. The regeneration results of CHF demonstrated a good reusability of this hydrogel fiber adsorbent, as the removal capacity was maintained at 80% after five recycling times.

Thus, being developed from a naturally available cellulose source, such as *Nypa fruticans* shell, this material could be a potential low-cost, non-toxic fiber-shaped adsorbent, with high regeneration and rapid saturation rates. Also, future investigations should be directed towards examining whether different diameters of the CHF and different polymer concentrations during its preparation could influence positively the dye removal ability of the adsorbent.

ACKNOWLEDGMENT: This study was financially supported by Van Lang University, Vietnam.

REFERENCES

[1] G. C. Silva, V. S. Ciminelli, A. M. Ferreira, N. C. Pissolati, P. R. P. Paiva *et al*., *Mater. Res. Bull*., **49**, 544 (2014), https://doi.org/10.1016/j.materresbull.2013.09.039

[2] J. Joseph, R. C. Radhakrishnan, J. K. Johnson, S. P. Joy, J. Thomas, *Mater. Chem. Phys*., **242**, 122488 (2020), https://doi.org/10.1016/j.matchemphys.2019.122488

[3] L. Liu, Z. Chen, J. Zhang, D. Shan, Y. Wu *et al*., *J. Water Process Eng*., **42**, 102122 (2021), https://doi.org/10.1016/j.jwpe.2021.102122

[4] S. Singh, V. C. Srivastava and I. D. Mall, *J. Phys. Chem. C*, **117**, 29 (2013), https://doi.org/10.1021/jp405289f

[5] G. Crini and E. Lichtfouse, *Environ. Chem. Lett*., **17**, 145 (2019), https://doi.org/10.1007/s10311-018-0785-9

[6] S. Rangabhashiyam, N. Anu and N. Selvaraju, *J. Environ. Chem. Eng*., **1**, 629 (2013), https://doi.org/10.1016/j.jece.2013.07.014

[7] M. T. Yagub, T. K. Sen, S. Afroze and H. M. Ang, *Adv. Colloid Interface Sci*., **209**, 172 (2014), https://doi.org/10.1016/j.cis.2014.04.002

[8] O. J. Rojas, "Cellulose Chemistry and Properties: Fibers, Nanocelluloses and Advanced Materials", Springer, 2016, vol. 271

[9] E. Sjöholm, K. Gustafsson, B. Eriksson, W. Brown and A. Colmsjö, *Carbohyd. Polym*., **41**, 153 (2000), https://doi.org/10.1016/S0144-8617(99)00080-6

[10] K. L. Tovar-Carrillo, S. S. Sueyoshi, M. Tagaya and T. Kobayashi, *Ind. Eng. Chem. Res*., **52**, 33 (2013), https://doi.org/10.1021/ie401793w

[11] K. Nakasone, S. Ikematsu and T. Kobayashi, *Ind. Eng. Chem. Res*., **55**, 30 (2016), https://doi.org/10.1021/acs.iecr.5b03926

[12] N. Srirachya, K. Boonkerd, L. Nakajima and T. Kobayashi, *Polym. Bull*., **75**, 5493 (2018), https://doi.org/10.1007/s00289-018-2341-y

[13] E. M. Ahmed, *J. Adv. Res*., **6**, 105 (2015), https://doi.org/10.1016/j.jare.2013.07.006

[14] G. R. Mahdavinia, A. Baghban, S. Zorofi and A. Massoudi, *J. Mater. Environ. Sci*., **5**, 330 (2014), https://www.jmaterenvironsci.com/Document/vol5/vol5_N2/39-JMES-422-2013-Mahdavinia.pdf

[15] T. Kamal, *Polym. Test*., **77**, 105896 (2019), https://doi.org/10.1016/j.polymertesting.2019.105896

[16] A. M. T. Jaworski, *Bio Design*, **2**, 3 (2014)

[17] L. S. Hamilton and D. H. Murphy, *Econ. Bot*., **42**, 206 (1988), https://doi.org/10.1007/BF02858921

[18] P. Tamunaidu and S. Saka, *Ind. Crop. Prod*., **34**, 1423 (2011), https://doi.org/10.1016/j.indcrop.2011.04.020

[19] M. El Alouani, S. Alehyen, M. El Achouri and M. H. Taibi, *MATEC Web Conf*., **149**, 02088 (2018), https://doi.org/10.1051/matecconf/201814902088

[20] R. G. Candido and A. R. Gonçalves, *Carbohyd. Polym*., **152**, 679 (2016), https://doi.org/10.1016/j.carbpol.2016.07.071

[21] A. Boonmahitthisud, L. Nakajima, K. D. Nguyen and T. Kobayashi, *J. Appl. Polym. Sci*., **134**, 10 (2017), https://doi.org/10.1002/app.44557

[22] Y. Zhou, M. Zhang, X. Hu, X. Wang, J. Niu *et al*., *J. Chem. Eng. Data*, **58**, 413 (2013), https://doi.org/10.1021/je301140c

[23] K. D. Nguyen, *Polymers*, **13**, 1909 (2021), https://doi.org/10.3390/polym13121909

[24] R. Bouhdadi, S. Benhadi, S. Molina, B. George, M. El Moussaouiti *et al*., *Maderas Cienc. Tecnol*., **13**, 1 (2011), http://dx.doi.org/10.4067/S0718-221X2011000100009

[25] M. Saber, L. El Hamdaoui, M. El Moussaouiti and M. Tabyaoui, *Cellulose Chem. Technol*., **56**, 69 (2022), https://doi.org/10.35812/CelluloseChemTechnol.2022.56.06

[26] O. Khelifi, I. Mehrez, W. B. Salah, F. B. Salah, M. Younsi *et al*., *LARHYSS J*., **28** (2016)

[27] J. Cheng, C. Zhan, J. Wu, Z. Cui, J. Si *et al*., *ACS Omega*, **5**, 5389 (2020), https://doi.org/10.1021/acsomega.9b04425

[28] T. T. C. Truong, N. T. T. Vo, K. D. Nguyen and H. M. Bui, *Cellulose Chem. Technol*., **53**, 573 (2019), https://doi.org/10.35812/CelluloseChemTechnol.2019.53.57

[29] F. M. Almutairi, Y. El-Ghoul and M. Jabli, *Polymers*, **13**, 3334 (2021), https://doi.org/10.3390/polym13193334